Available online at www.sciencedirect.com

ScienceDirect

Procedia Engineering 144 (2016) 982 – 989

Procedia Engineering

www.elsevier.com/locate/procedia

12th International Conference on Vibration Problems, ICOVP 2015

Uncertainty Quantification of Subcritical Nonlinear Aeroelastic system using Integrated Interpolation Method and Polynomial chaos expansion

Thanusha M.T[a], Sunetra Sarkar[b,*]

[a, b] *Department of Aerospace Engineering, Indian Institute of Technology, Madras, Chennai, 600036, India*

Abstract

The present paper is about analyzing and quantifying parametric uncertainties in a nonlinear aeroelastic system. The response surface of a subcritical system has discontinuities which makes it difficult to analyze using spectral approaches. A quadrature based spectral parametric uncertainty tool called nonintrusive spectral projection (NISP) can capture discontinuities in the response surface only by infinite number of points. As the number of random variable increases, the order of expansion has to increase drastically in order to capture the response accurately. Hence an alternate approach using integrated interpolation scheme which was earlier applied for a thermoacoustic problem is being applied to a classical flutter problem. It is found to be accurate and computationally cheaper than traditional Monte Carlo simulations (MCS) in capturing the response surface. This paper intends to apply the interpolation scheme to the nonlinear aeroelastic model and compares it with quadrature based polynomial chaos expansion (PCE) approach and MCS.

Peer-review under responsibility of the organizing committee of ICOVP 2015

Keywords: Subcritical; aeroelastic; response surface interpolation

1. Introduction

An Aeroelastic phenomenon occurs when there is an interaction between aerodynamic, elastic and inertial forces. Such kind of fluid structure interaction can lead to instability and vibration problems. A very good example of

* Corresponding author
E-mail address: thanushreya@yahoo.co.in ; sunetra.sarkar@gmail.com

Peer-review under responsibility of the organizing committee of ICOVP 2015
doi:10.1016/j.proeng.2016.05.128

dynamic aeroelasticity would be flutter. Flutter is determined from conditions which give either a divergent or limited amplitude response[1]. For a simplified linear system there exists a critical reduced velocity or flutter point at which the system becomes unstable and undergoes divergent oscillations, leading to failure of the structure[2] . In a real case situation, flutter problems can be solved by taking nonlinearity into consideration. Breitbach [3] has investigated various kinds of nonlinearities that can affect an aircraft structure, which are distributed and concentrated nonlinearities. The flutter point of the system change when uncertainty is introduced and hence play an important role in designing aircraft wings and control surfaces. Generally, uncertainties are divided into two categories; aleatory and epistemic[4,5]. Aleatory uncertainty represents the inherent randomness in the system parameter and is irreducible whereas epistemic uncertainty describes subjectivity, ignorance or lack of information in any phase of the modeling process. It is reducible because it can be decreased with an increased knowledge or by collecting more data. Uncertainties in an aeroelastic system include system modeling, measurement inaccuracies, structural properties and operating environment. Among these uncertainties, randomness in structural properties and operating environment come under aleatory category. The present study focuses on interaction of nonlinearities of aeroelastic systems with parametric uncertainties.

The effect of freeplay, hysteresis and cubic nonlinearities on flutter was initially investigated by Woolston et al., [6] using analog computing and wind tunnel experiments. Structural nonlinearities typically arise from freeplay at the interconnections between different components, worn hinges, loose linkages etc. Limit Cycle Oscillations (LCO) and chaotic motions were reported in experiments with freeplay in pitch using low speed wind tunnel [7,8]. According to Tang and Dowell, for nonlinear systems the flutter instability behavior not only depends on structural and aerodynamic parameters but also on initial conditions [7].

Cubic nonlinearities in 2 degree-of-freedom (2DOF) aerofoil change the behavior of the system at flutter point. For a hard spring, the nonlinear flutter boundary is independent of initial conditions. Instead of divergent flutter, a limit cycle oscillation occurs for velocities greater than the flutter speed. For a soft spring, it was found that the initial condition can trigger oscillations below the linear flutter speed. Lee et al. [9–11] has illustrated the destabilizing effect of a soft spring which shows that flutter can be induced at a velocity below the linear flutter velocity .

Uncertainty quantification method is selected based on the information available about the uncertain parameters. This information can be acquired through data-bases, experiments, expert knowledge etc. If the probability distribution of the uncertain parameter is known, then the response of the system can be determined by using the theory of probability and random process[12]. This idea is implemented in methods such as Monte Carlo simulation, spectral methods, response surface method etc. The polynomial chaos expansion is a spectral method in which the input is represented by employing orthogonal polynomial as the basis in a random space [13,14]. A classical Galerkin-PCE approach which is intrusive in nature modifies the governing equations to a coupled form in terms of chaos coefficients. This increases the complexity of the system and becomes computationally expensive. To reduce the intricacy several uncoupled variants of polynomial chaos expansion such as probabilistic collocation method by Loeven et al.[15] is used, where the problem is collocated at Gauss quadrature points in the probability space. The deterministic runs were then performed at these collocation points which resulted in an exponentially fast convergence [16,17]. For multiple random variables, the collocation grids are constructed using tensor product of the one-dimensional grid. This increases the number of collocation points and as an alternative, sparse grid collocation approach was implemented [18–20].

The nonlinear aeroelastic system considered here exhibits subcritical bifurcation with a discontinuous behavior in the response surface. Similar kind of a system was solved by B-Spline interpolation technique by Millman et al.[21], but it smoothened out the discontinuities by drawing piecewise linear B-splines giving erroneous response. Hence an integrated interpolation scheme which uses a combination of linear and proximal interpolations is employed [22]. It is based on equi-probable nodes, which uses the idea of equal probability of the nodes giving least error. This scheme is non intrusive and can be applied to any number of random dimensions.

2. Methodology

The nonlinear aeroelastic system used for the simulation is shown in Fig. 1:

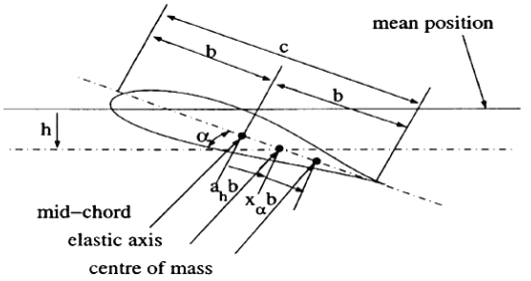

Fig. 1. The schematic of an aerofoil with pitch (α) and plunge (h) degrees-of-freedom

The governing equations for a nonlinear aeroelastic system used for the simulation are [9]:

$$\xi'' + x_\alpha \alpha'' + 2\zeta_\xi \frac{\bar{\omega}}{U^*}\xi' + \left(\frac{\bar{\omega}}{U^*}\right)^2 (\xi) = -\frac{1}{\pi\mu} C_L(\tau) \tag{1}$$

$$\frac{x_\alpha}{r_\alpha}\xi'' + \alpha'' + 2\frac{\zeta_\alpha}{U^*}\alpha' + \left(\frac{1}{U^*}\right)^2 (\alpha + \beta_\alpha \alpha^3 + \gamma_\alpha \alpha^5) = \frac{2}{\pi\mu r_\alpha{}^2} C_M(\tau) \tag{2}$$

where $\xi = h/b$ is the non-dimensional plunge displacement of the elastic axis, β_α is the ratio of cubic spring constant to linear spring constant in pitch. The response i.e., α (radians) gives supercritical Hopf bifurcation when β_α is positive whereas for softening nonlinearity the response gives subcritical bifurcation. r_α is the radius of gyration about the elastic axis, ζ_ξ and ζ_α are the viscous damping co-efficients in plunge and pitch respectively. The elastic axis is located at a distance $a_h b$ from the mid-chord and the centre of mass is located at a distance $x_\alpha b$ from the elastic axis. In the above equation $U^* = \bar{U}/(b\omega_\alpha)$ is the nondimensional velocity or reduced velocity. $\bar{\omega} = \omega_\xi/\omega_\alpha$ where ω_ξ and ω_α are the uncoupled plunging and pitching modes natural frequencies. The $(')$ denotes differentiation with respect to nondimensional time τ defined as $\tau = Ut/b$. $C_L(\tau)$ and $C_M(\tau)$ are the lift and pitching moment coefficients whose expression is given by Fung [23]; they contain indicial integral forms in terms of Wagner's functions and are transformed into a set of eight ODEs in time domain. The parameters and the non-dimensionalization used here are as shown in Lee et al. [9].

While dealing with subcritical systems, the response tends to diverge beyond bifurcation point for any initial conditions except $\alpha_0 = 0$, hence to regain the stability and understand the system better, a fifth order nonlinearity is applied in pitching mode for the present study.

3. Simulation methods

Here a 2DOF subcritical aeroelastic system is simulated using Monte Carlo method, polynomial chaos method and integrated interpolation scheme. The deterministic non-dimensional linear flutter velocity for the system was found to be 6.2865. When nonlinearity was induced in the system using a soft cubic spring in pitch, the response became unstable beyond the same reduced velocity as the linear flutter velocity. This behavior was also reported by Lee et al. [9], thus validating the present deterministic code. The bifurcation behavior of the response is shown in figure 2 for varying nondimensional velocity U* as the bifurcation parameter. The value of fifth order spring coefficient was chosen such that the response does not go beyond stall angle and simulation was fixed at β_α =-3 to ensure subcritical behavior. It includes all the possible values of initial conditions and is found that for certain initial conditions the system gives damped response and for others it gives limit cycle oscillations. As the velocity is increased, the response went from damped to LCO at U* equal to 6.2865 which was same as linear bifurcation

velocity. When the system was forced to bring down the response from LCO to stable solution by decreasing the velocity, the bifurcation point moved to 6.16. This kind of hysteresis is observed in the simulation and was found in experiments conducted by Bunton and Denagri [24]. In the figure, A-B is the stable branch in which any initial condition will give damped behavior; C-D depends on initial condition and goes to limit cycle oscillations (LCO). The branch B-C (hypothetical branch) marks the unstable LCO of the subcritical Hopf bifurcation behavior. Therefore the subcritical region lies in between these two points (B-C) which can give two stable solutions depending on the initial condition.

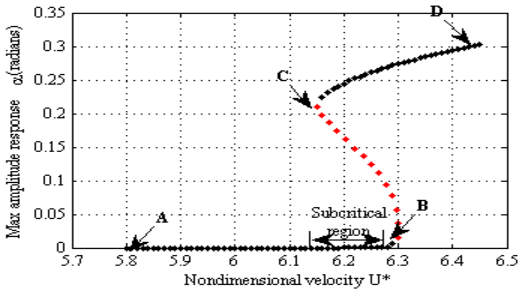

Fig. 2. Bifurcation diagram of a 2DOF subcritical system for $\beta_\alpha = -3$

3.1. Polynomial Chaos Expansion

As the reference for the present study, Monte Carlo simulations (MCS) are used for both polynomial chaos expansion and integrated interpolation scheme. MCS is carried out for two single random variable cases; cubic spring constant (β_α) and initial condition (α_0) and for two random variables (β_α and α_0). These parameters are assumed to be independent Gaussian random variables. The accuracy of this method depends on the number of samples hence time, computational power and memory required for the iterations are more [25,26]. A non-intrusive projection method of polynomial chaos expansion method was useful in getting accurate results in the case of supercritical Hopf bifurcation which has continuous change in response. Time required for this simulation was drastically less when compared to MCS. Here probabilistic Hermite polynomial is used for approximating Gaussian input random variable. According to the order of the polynomial (p), (p+1) collocation points are found through Gauss Hermite quadrature rule. Deterministic runs are performed on these points in the governing equations and are used to find the polynomial coefficients $\hat{\alpha}(x,t)$ through the projection formula. After which, the final response is expanded through the series:

$$R(x,t,\xi) = \sum_{i=0}^{n} \hat{\alpha}(x,t)\varphi_i(\xi) \tag{3}$$

where φ is the probabilistic hermite polynomial and ξ is the standard normal random variable used for calculating the input parameter. The number of terms in the expansion (n) is given by

$$n = \frac{(p+l)!}{p!l!} \tag{4}$$

where l is the number of random variables. MCS were carried out for 10,000 samples in order to predict the behavior and is used as a reference solution. Fig. 3 shows both MCS and PCE simulations for a subcritical system. The response surface by MCS is shown in Fig. 3(a); the sharp changes in the response between the damped solution and the LCO can be clearly seen. It has also been captured well in the cumulative distribution function (CDF) plot presented in Fig. 3(b). Fig. 3(c) and 3(d) shows response α (radians) and CDF using PCE. The polynomial order chosen for the simulation was 25 with 26 collocation points. Fig. 3(c) shows an oscillatory behavior in the limited amplitude responses which are not characteristic of the system and does not change much by increasing the polynomial order. The collocation points are out of the physical boundary of the system while using Hermite quadrature which gives unrealistic solution. The increasing slope in Fig. 3(d) shows varying LCO values which are

not feasible in subcritical systems. In order to capture the discontinuity, large number of chaos expansion terms is required which increases the polynomial order to infinity. But still it can be seen that the response is captured only partially and fails to predict the discontinuous nature of the system. Hence another alternative approach based on interpolation technique was used to capture the discontinuities of the subcritical system more accurately and efficiently.

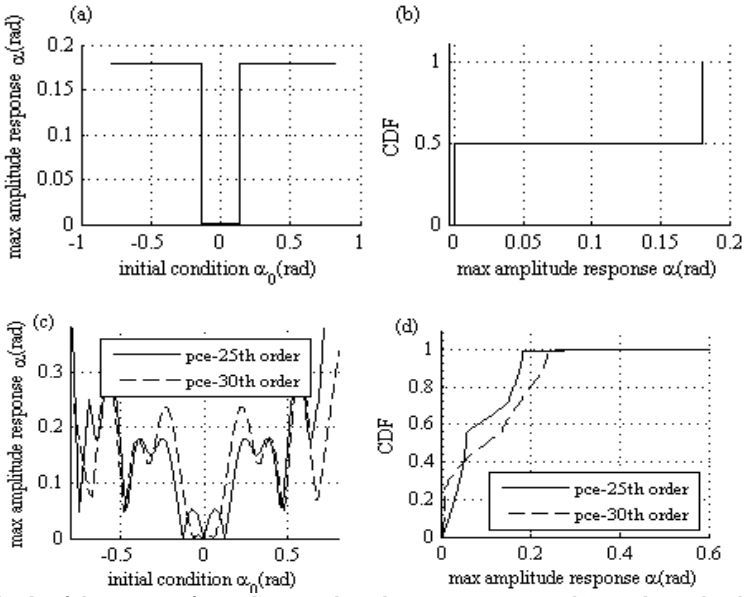

Fig 3.(a) maximum amplitude of the response for random initial condition α0 using MCS (b) cumulative distribution function (CDF) of the response using MCS (c) maximum amplitude of the response for random initial condition α0 using PCE (d) cumulative distribution function (CDF) of the response using PCE

3.2. Integrated Interpolation Scheme (IIS)

Because of the above flaws in PCE an algorithm based on interpolation which uses a combination of linear and proximal interpolation is used. In nearest neighbour or proximal interpolation the value at a particular response point is the value of the nearest response grid point. This ensures that the output remains as characteristic of the system and hence it is specifically used in the discontinuous region. Linear interpolation is applied at all the other regions of the subcritical system. A key element of this method is the use of equiprobable nodes, on which deterministic runs are performed and then interpolation scheme is applied. As the number of nodes required for IIS scheme is less, it drives the simulation faster, thus giving an advantage over Monte Carlo simulation and can be used for multirandom variables.

3.2.1 Equiprobable nodes

The interpolation nodes used for IIS are equiprobable nodes. To obtain the nodes let's consider a Gaussian input distribution whose interval lies between -∞ to +∞. But 99% of the data lies between the ranges -4 to +4 of the Gaussian probability density function:

$$\left(\frac{1}{\sqrt{2\pi}}\right)^2 \int_{-4}^{4}\int_{-4}^{4} e^{-\left(\frac{\xi_1^2+\xi_2^2}{2}\right)} d\xi_1\, d\xi_2 = 0.9991 \tag{5}$$

Hence -4 to 4 interval is selected for the single random variable and for two random variable case ξ_1 and ξ_2. The area of the probability distribution curve of the standard normal variable is then divided into equal number of parts and the abscissa corresponding to the interval gives the location of the equiprobable nodes. As the name suggests the

equiprobable node confirms that the probability of a given set of random numbers lying in any of the node intervals is the same. A random input has equal probability to lie in the interval of discontinuity or any other interval. This ensures that the nodes give best approximation of the response.

For a two dimensional random variable case a mesh grid of the same nodes are taken in each direction. Fig. 4(a) and 4(b) shows the mesh grid distribution of MCS and IIS respectively.

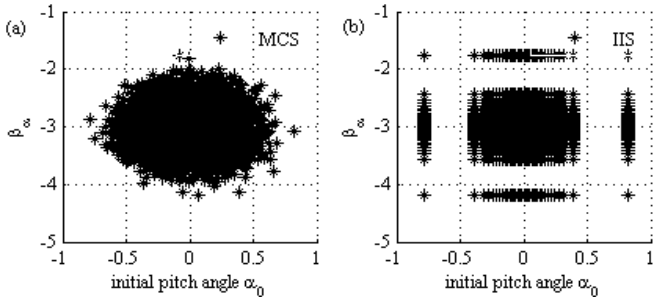

Fig. 4. (a) Samples of β_α and α_0 for MCS (b) mesh grid of equiprobable nodes of β_α and α_0

4. Results

4.1 Single random variable case

The simulations are run for random initial pitch angle, for $\tilde{\alpha} = 0$ and $\sigma_\alpha = 0.2$. Here proximal interpolation is used at the discontinuity and linear interpolation for the rest of the region respectively. The result can be further improved by increasing the number of nodes in the discontinuous region rather than increasing the number of equiprobable nodes. Thus the number of nodes required for the model was 20 with 10 additional collocation points at the region of discontinuity. The simulations were carried out for 6000 seconds to stabilize the response surface. The cumulative distribution function (CDF) and probability density function (PDF) of the response α(radians) for the present scheme are compared to the reference solution as shown in Fig. 5(a) and 5(b). The probability of the response (PDF) and CDF are found using histogram in Matlab. From Fig. 5(c) it can be seen that the system has both damped oscillation or zero amplitude and a limit cycle oscillation of 0.18radians or 10.3^0. All the simulations were carried out with nondimensional velocity of 6.21 which is within the subcritical range. The time required to produce same result with integrated interpolated scheme was almost 1/100th of MCS.

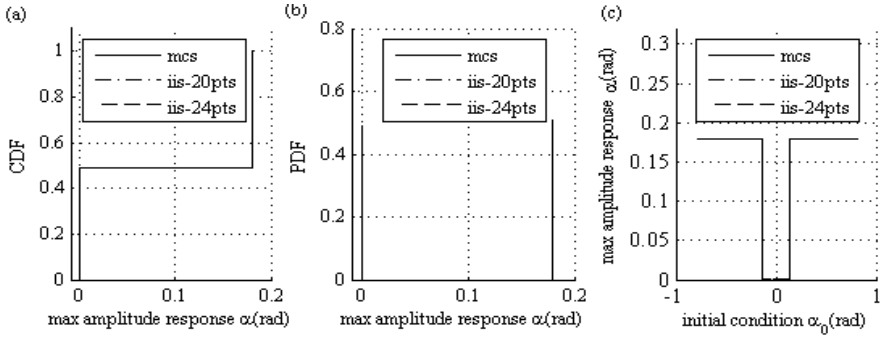

Fig. 5. (a) CDF of response with 10000 MCS runs and IIS with 20 and 24 node interpolation (b) PDF of response with 10000 MCS runs and IIS (c) Response surface with 10000 MCS runs and IIS

Similar to α_0, the softening cubic spring constant β_α is assumed to be random and of Gaussian distribution. Simulations are carried out with mean value of β_α as -3 and standard deviation as 0.3 respectively for constant initial pitch angle of 11deg to ensure that LCO has developed. All the other parameters are same as the previous case. Here 26 equiprobable nodes were required in order to match the reference solution. From Fig. 6(a) and 6(b) it can seen that the maximum amplitude of the response varies with β_α hence the number of nodes required to capture

the response has increased slightly than initial condition (α_0) case. Again 10 additional collocation points were added for a better approximation of the discontinuous region as shown in Fig. 6(c). Since the deterministic runs are performed only at these nodes, the time taken for this simulation was almost same as the previous case. The PDF shows two peaks where the first one represent the stable solution and the second peak forms a Gaussian curve, due to varying stable periodic response. Good agreement has been achieved between MCS and IIS.

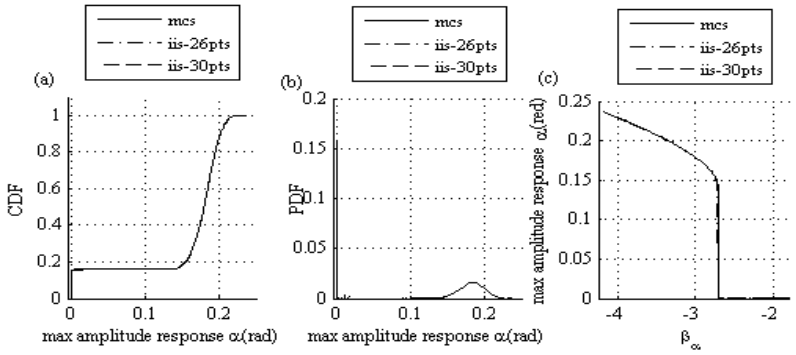

Fig. 6.(a) CDF of response with 10000 MCS runs and IIS with 26 and 30 node interpolation (b) PDF of response with 10000 MCS runs and IIS (c) Response surface with MCS and IIS

4.2 Two random variable case

Here the initial pitch angle and cubic spring constant in pitch are considered to be independent Gaussian random variables. The mean and standard deviation of the variables are same as the previous cases.

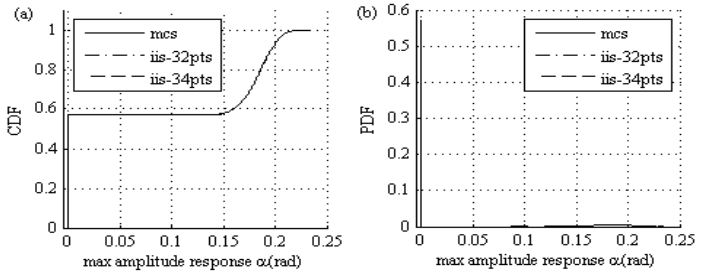

Fig. 7. (a) CDF of MCS and IIS (b)PDF of MCS and IIS

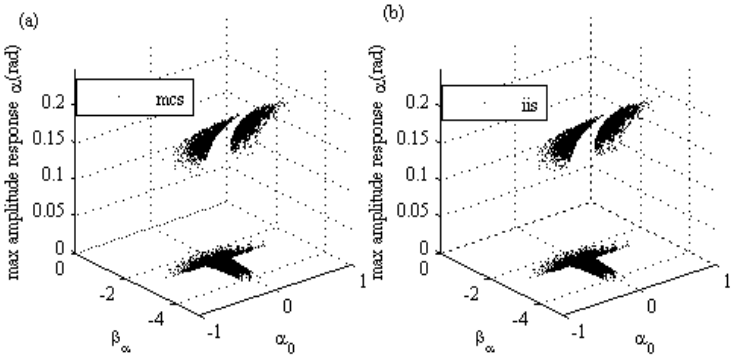

Fig. 8. Response surface of (a) 10000 samples of MCS (b) 34 equidistant nodes of IIS

In this case 32 equiprobable nodes are used along α_0 and β_α dimension and a mesh grid is formed for the

simulation. Additional 20 collocation points were added for a better approximation of the discontinuous region. The CDF and PDF in this case are as shown in Fig. 7(a) and 7(b) respectively. From the plot it can be seen that the response surface of IIS resemble MCS very closely. In a two random variable case also the LCO values vary according to the cubic spring constant. Hence both the plots are similar to cubic spring single random variable case.

A 3D response plot for MCS and IIS for a two random variable case is shown in Fig. 8(a) and 8(b). The discontinuity of the system is visible along α_0 axis whereas the response changes from stable solution to varying LCO in the negative direction of β_α .

5. Conclusion

Numerical simulations were carried out for a 2DOF aeroelastic subcritical system using various methods of uncertainty quantification, among which the integrated interpolation scheme with equiprobable node distribution was found to be very efficient in capturing discontinuities exhibited by the system. The advantages of using IIS for discontinuous response surface are highlighted in the present work. The PDF and CDF of the response are compared with the reference MCS solution and good agreement is found between MCS and IIS when compared to PCE. The polynomial chaos expansion a class of spectral method was unable to capture the response accurately and showed characteristics which are not feasible in the system. The proposed scheme can be used with any input distribution and also for multirandom variable case with least error and less computational time.

References

[1] B.H.K. Lee, P. Leblanc, Flutter analysis of a two-dimensional airfoil with cubic non-linear restoring force, National research council of Canada, aeronautical note nae-an-36, nrc no. 25438, 1986.
[2] R.M. Laurenson, R.M. Trn, Flutter Analysis of Missile Control Surfaces Containing Structural Nonlinearities, AIAA J. 18 (1980) 1245–1251. doi:10.2514/3.50876.
[3] E. Breitbach, Effect of structural nonlinearities on aircraft vibration. AGARD of NATO, (1977).
[4] R.E. Melchers, Structural reliability analysis and prediction, John Wiley & Sons, West Sussex, England, 2 edition (1999).
[5] A. Der Kiureghian, O. Ditlevsen, Aleatory or epistemic? Does it matter?, Struct. Saf. Volume 31, Issue 2, Pages 105–112 (2009).
[6] D. Woolston, Runyan HL Andrews RE, An Investigation of Effects of Certain Types of Structural Nonlinearities on Wing and Control Surface Flutter. Journal of Aeronautical Sciences, Vol. 24, No. 1, J. Aeronaut. Sci. 1957, 24 57-63.
[7] D. Tang, E. Dowell, Comparison of theory and experiment for non-linear flutter and stall response of a helicopter blade, J. Sound Vib. 165(2),251-276 (1993).
[8] Z. Yang, L. Zhao, Analysis of limit cycle flutter of an airfoil in incompressible flow, J. Sound Vib. 123(1), 1-13 (1988).
[9] B.H.K. Lee, L.Y. Jiang, Y. S Wong, Flutter of an airfoil with a cubic nonlinear restoring force. AIAA-98-1725(1998)
[10] S. Price, H. Alighanbari, B. Lee, The aeroelastic response of a two-dimensional airfoil with bilinear and cubic structural nonlinearities, J. Fluids Struct. 9, 175–193 (1995).
[11] B. Lee, L. Gong, Y. Wong, Analysis and computation of nonlinear dynamic response of a two-degree-of-freedom system and its application in aeroelasticity, J. Fluids Struct. 11, 225–246 (1997).
[12] I. Elishakoff, R. Haftka, J. Fang, Structural design under bounded uncertainty—optimization with anti-optimization, Comput. Struct. Volume 53 no.6, pp.1401–1405 (1994).
[13] R. Ghanem, P. Spanos, Stochastic finite elements: a spectral approach, Newblock Springer-Verlag, New York (1991).
[14] D. Xiu, G. Karniadakis, Modeling uncertainty in flow simulations via generalized polynomial chaos, J. Comput. Phys. Volume 187, Issue 1, 1 May, Pages 137–167 (2003).
[15] G. Loeven, J. Witteveen, H. Bijl, Probabilistic collocation: an efficient non-intrusive approach for arbitrarily distributed parametric uncertainties, Proc. 45th AIAA …. (2007).
[16] S. Hosder, R. Walters, R. Perez, A non-intrusive polynomial chaos method for uncertainty propagation in CFD simulations, Proceedings of the 44th AIAA Aerospace Sciences Meeting and Exhibit, AIAA paper 2006{891, Reno, January (2006).
[17] R. Ghanem, Stochastic finite elements with multiple random non-Gaussian properties, J. Eng. Mech. (1999).
[18] Smolyak, S.: Quadrature and interpolation formulas for tensor products of certain classes of functions, Soviet Math. Dokl., 4 ,240-243(1963).
[19] C. Pettit, P. Beran, Spectral and multiresolution Wiener expansions of oscillatory stochastic processes, J. Sound Vib. (2006).
[20] D. Xiu, Efficient collocational approach for parametric uncertainty analysis, Commun. Comput. Phys. Vol. 2, No. 2, pp. 293-309 (2007).
[21] D. Millman, P. King, R. Maple, P. Beran, Predicting uncertainty propagation in a highly nonlinear system with a stochastic projection method, AIAA Pap. (2004).
[22] V. Nair, S. Sarkar, R. Sujith, Uncertainty quantification of subcritical bifurcations, Probabilistic Eng. Mech. 34, 177-188 (2013).
[23] Y.C. Fung, An Introduction to the Theory of Aeroelasticity. John Wiley & Sons, Inc., New York. (1955)
[24] R. Bunton, C. Denegri, Limit cycle oscillation characteristics of fighter aircraft, Journal of Aircraft, 37(5), 916–918 (2000).
[25] R. Rubinstein, Simulation and the Monte Carlo method, Wiley series in probability and statistics (1981).
[26] I. Sobol, The Monte Carlo method, Mir publishers, Moscow, 1984.